Clays and Clay Minerals, Vol. 54, No. 6, 721–736, 2006.

CLAY-SIZED MINERALS IN PERMAFROST-AFFECTED SOILS (CRYOSOLS) FROM KING GEORGE ISLAND, ANTARCTICA

FELIPE N. B. SIMAS[1,*], CARLOS ERNESTO G. R. SCHAEFER[2], VANDER F. MELO[3], MARCELO B. B. GUERRA[2], MARTIN SAUNDERS[4] AND ROBERT J. GILKES[5]

[1] Mestrado em Meio Ambiente e Sustentabilidade, UNEC – Centro Universitário de Caratinga, Av. Moacyr de Mattos, Centro, Caratinga, 35300-000, Minas Gerais, Brazil
[2] Departamento de Solos – Universidade Federal de Viçosa, Av. PH Rolfs s/n, Viçosa, 36570-000, Minas Gerais, Brazil
[3] Departamento de Solos e Engenharia Agrícola – Universidade Federal do Paraná, Rua dos Funcionários, 1540 - Juvevê 80035-070 - Curitiba – Paraná, Brazil
[4] Centre for Microscopy and Microanalysis – The University of Western Australia, Nedlands, WA, 6009, Australia
[5] School of Earth and Geographical Sciences, The University of Western Australia, Nedlands, WA, 6009, Australia.

Abstract—Cryosols from Maritime Antarctica have been less studied than soils from continental areas of Antarctica. In this work X-ray diffraction, difference X-ray diffraction, differential thermal analysis, thermogravimetry, transmission electron microscopy/energy dispersive spectroscopy and selective chemical dissolution were used to characterize the clay fraction of basaltic, acid sulfate and ornithogenic Cryosols from ice-free areas of Admiralty Bay, King George Island. Non-crystalline phases are important soil components and reach >75% of the clay fraction for some ornithogenic soils. Randomly interstratified smectite-hydroxy-Al-interlayered smectite is the main clay mineral of basaltic soils. Kaolinite, chlorite and regularly interstratified illite-smectite predominate in acid sulfate soils. Jarosite is also an important component of the clay fraction in these soils. Crystalline Al and Fe phosphates occur in the clay at sites directly affected by penguin activity and the chemical characteristics of these ornithogenic sites are controlled by highly reactive, non-crystalline Al, Si, Fe and P phases. Chemical weathering is an active process in Cryosols in Maritime Antarctica and is enhanced by the presence of sulfides for some parent materials, and faunal activity.

Key Words—Allophane, Clay Minerals, Cryosols, Maritime Antarctica, Ornithogenesis, Phosphate, Soils, X-ray Amorphous Phases.

INTRODUCTION

Most pedological studies in Antarctica have dealt with soils from extremely cold and dry continental areas where physical weathering accounts for the rather incipient soil development (Kelly and Zumberge, 1961; Campbell and Claridge, 1987, 2004a, 2004b; Bockheim and Tarnocai, 1998). Soils from Maritime Antarctica have received much less attention. In this part of Antarctica, warmer temperatures, the greater availability of liquid water, the widespread presence of bird colonies, pronounced vegetation development and greater soil microbial activity result in more developed soils.

Some authors have stated that under these conditions chemical weathering is an important soil-forming process leading to considerable amounts of pedogenic Fe oxides, phosphates and clay minerals (Tatur and Barczvk, 1985; Tatur, 1989; Blume *et al*., 2002, 2004; Simas *et al*., 2005 under review). Other authors concluded that even under maritime conditions chemical weathering is insignificant and have attributed the formation of clay minerals to hydrothermal alteration of parent materials and eolian inputs from nearby active volcanoes (Jeong and Yoon, 2001; Yong *et al*., 2004). Clearly our understanding of soil formation in Maritime Antarctica is still limited.

Due to their large specific area, clay-sized minerals greatly influence soil physical and chemical properties, even when they are present in small amounts. Various environmental issues, such as the influence of acid deposition on soils, retention and cycling of organic and inorganic contaminants, nutrient availability and organic C dynamics, are strongly related to clay formation. This is of particular importance in Antarctica where there is increasing impact of local and global human activities on these fragile ecosystems. In this paper, we have studied in detail the clay fraction from the main soil types at Admiralty Bay, King George Island.

MATERIAL AND METHODS

Study area

Admiralty Bay (62º03′40′′–62º5′40′′ S and 58º23′30′′–58º24′30′′ W) is located in King George Island and is part of the South Shetlands Archipelago, Maritime Antartica (Figure 1). Data sets from 1982–2002, acquired at the Brazilian Comandante

* E-mail address of corresponding author:
fsimass@yahoo.com.br
DOI: 10.1346/CCMN.2006.0540607

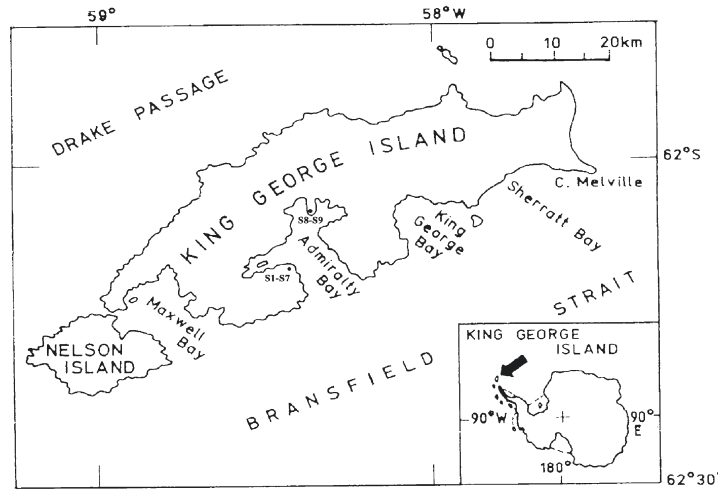

Figure 1. King George Island and the locations of the sites studied at Admiralty Bay (S1−S9) (modified from Birkenmayer, 2001).

Ferraz Station, report mean air temperatures varying from −6.4ºC in July to +2.3ºC in February. Mean annual precipitation is 366.7 mm. Positive air temperatures occur from November until March when effective precipitation as liquid water is increased due to melting of accumulated winter snow. Soils have formed predominantly from tholeite basalts and, to a lesser extent, from sulfide-bearing andesites and related moraine, solifluction and fluvioglacial deposits. Intense paleohydrothermal activity (Yong *et al*., 2004) and recent eolian deposition of volcanic ash in this part of Antarctica have been reported (Blume *et al*., 2004; Yong *et al*., 2004).

Site characteristics and soil sample treatments

We selected two altitudinal sequences ranging from upland, ahumic soils to lower, acid, ornithogenic soils with greater organic C contents, as well as acid soils formed from sulfide-bearing rocks and related deposits. Soil pH, nutrient availability, exchangeable Al and particle size distribution were determined for <2 mm samples (EMBRAPA, 1997). Total organic C was determined on <0.5 mm samples by wet combustion (Yeomans and Bremner, 1988). General site descriptions and their approximate location are presented in Table 1 and Figure 1, respectively. Some important chemical and physical characteristics of the soils are presented in Table 2. The clay fraction was separated by dispersion in water at pH 10.0 (1 g Na_2CO_3: 10 L of deionized water), sieving of the sand fraction and sedimentation of silt + clay followed by siphoning of the <2 μm fraction (Gee and Bauder, 1986).

Based on their general chemical properties, which are greatly influenced by parent materials and bird detritus, the soils are grouped as follows:
Group 1: basaltic soils − sites 1 and 2
Group 2: ornithogenic soils − sites 3, 4, 5, 6 and 7
Group 3: acid sulfate soils − sites 8 and 9

Chemical dissolution

The use of selective dissolution for mineralogical studies has been much reported in the literature (Campbell and Schwertmann, 1985; Smith, 1994; Melo *et al*., 2002a). In this study, natural (untreated) clay samples were submitted to the following sequential extraction:
(1) pH 10.0 Na pyrophosphate (pyr) − extraction of Al and Fe bound to organic matter (Dahlgren, 1994);
(2) pH 3.0 0.2 mol/L ammonium oxalate in the dark (ox) − extraction of poorly ordered Fe, Al and Si compounds (Schwertmann, 1973);
(3) 0.5 mol/L NaOH (OH) − extraction of poorly ordered aluminosilicates not removed by the previous extractions (Jackson *et al*., 1986, modified by Melo *et al*., 2002a, 2002b).

The general procedure for all extractions was: (a) drying of the samples at 105ºC for 12 h before and after each extraction to obtain initial and final weights to 0.0001 g; (b) removal of excess salt by washing with 0.5 M $(NH_4)_2CO_3$ and deionized water after each extraction; (c) Al, Fe, Si, Mg and Ca in the extracts were determined by inductively coupled plasma-mass spectrometry (ICP-MS) with the results converted to percentage oxides. The P concentration was determined in the oxalate and NaOH extracts by photocolorimetry and is expressed as P_2O_5. The total mass removed by each treatment for an initial mass of 1000 g is as follows:

$T_i = Y_i + X_i + Z_i$ where:

T_i = total mass removal for sample i (g/kg);
Y_i = removal by pyrophosphate extraction (g/kg);
X_i = (0.001*removal by oxalate extraction (g/kg))* $(1000-Y_i)$;
Z_i = (0.001*removal by NaOH extraction (g/kg))* $(1000-(X_i+Y_i))$.

Table 1. General characteristics of the sites studied.

Site	Altitude (m a.s.l.*)	Vegetation	Site description
Group 1 – Basaltic soils			
Site 1	147	Absent	Subpolar desert with no ornithogenic influence and no vegetation.
Site 2	90	U	Well drained, no ornithogenic influence, sparse vegetation.
Group 2 – Ornithogenic soils			
Site 3	72	D > C	Abandoned penguin rookery on the highest level of ornithogenic influence; probably the most ancient level of ornithogenic soils; well developed, continuous vegetation. Permafrost at 50 cm.
Site 4	69	D > M > C	Abandoned, well drained penguin rookery; phosphatization evidenced by discontinuous whitish horizons throughout the profile; well developed, continuous vegetation. Permafrost at 50 cm.
Site 5	32	M > D	Poorly drained. This site receives a large amount of leachate from the upslope ancient rookeries; well developed continuous vegetation.
Site 6	63	M > D > U > C	Well drained. Indirect ornithogenic influence through lateral leacheate. Exuberant vegetation cover. Abundant roots down to 25 cm. Fibric O horizon from 0–10 cm.
Site 7	61	M > D > U > C	Well drained, similar to site 6. Buried O horizon at 30–40 cm.
Group 3 – Acid sulfate soils			
Site 8	69	Rare crustose lichens	Shallow profile, lithic contact at 35 cm. Basaltic colluvium overlying yellowish, acidic material.
Site 9	47	U > M > D	Stable terminal moraine. Whole profile affected by sulfates. Representative of soils formed from sulfide-affected rocks of Keller Peninsula. Permafrost at 40 cm.

D – *Deschampsia Antarctica* (Gramineae); C – *Colobanthus quitensis* (Cariofilaceae); M – mosses; U – *Usnea sp.* (lichen)
* metres above sea level

Table 2. Some chemical and physical characteristics of the soils studied.

Depth (cm)	pH[1]	P[2] (mg/kg)	Al[3] ($cmol_c/dm^3$)	TOC[5] (g/kg)	csand	fsand	silt	clay
					(dg/kg)			
Site 1								
0–20	6.8 (0.3)	56.6 (11.9)	0.3 (0.2)	1.0	49.5	21.0	25.0	15.0
Site 2								
0–50	7.1 (0.7)	516.5 (58.5)	0.2 (0.2)	3.2 (4.3)	33.0	8.6	35.6	22.8
Site 3								
10–50	4.2 (0.1)	1015.3 (267.4)	10.5 (2.5)	6.0 (2.7)	59.2	13.4	19	8.5
Site 4								
0–70	4.1 (0.3)	1421.8 (310.3)	6.2 (1.5)	13.0 (2.3)	80.5	5.0	7.5	7.0
Site 5								
0–40	5.1 (0.5)	391.0 (102.0)	6.2 (3.3)	20.5 (18.6)	73.6	5.3	8.1	24.3
40–50	4.9	826.2	3.3	8.0	74.0	6.4	11.8	10.2
Site 6								
10–40	4.0 (0.1)	1049.9 (55.7)	6.5 (0.7)	32.7 (6.1)	50.0	16.3	25.7	8.0
Site 7								
0–20	4.5 (0.1)	726.9 (14.0)	3.9 (0.5)	66.0 (16.9)	72.0	3.0	14.0	11.0
20–40	4.3 (0.1)	1140.1 (238.0)	5.0 (0.7)	100.0 (9.9)	68.0	8.0	14.0	10.0
Site 8								
0–10	7.6	173.5	0.0	4.0	29.0	8.0	34.0	29.0
20–30	4.7 (0.2)	36.7 (13.8)	17.1 (1.2)	1.0	20.0	6.0	72.0	2.0
Site 9								
0–10	5.1	44.6	7.6	5.0	52.0	6.0	26.0	16.0
20–70	4.5 (0.3)	21.3 (4.0)	27.7 (7.3)	1.2 (0.4)	29.2	7.2	64.0	1.0

[1] 1:2.5 water; [2] Melich-1 extractable-P; [3] exchangeable Al^{3+}; [4] Total organic C
( ) standard error

X-ray diffraction and difference XRD

Approximately 0.5 g of finely ground dry clay samples were mounted on aluminum holders and submitted to X-ray diffraction (XRD) analysis. The XRD patterns were obtained before and after each extraction, following the procedure proposed by Schulze (1994). Difference XRD (DXRD) patterns were obtained by subtracting the pattern for a treated sample from the XRD pattern obtained prior to the treatment (untreated sample – pyr, pyr-ox and ox-OH) (Campbell and Schwertman, 1985; Schulze, 1994).

Oriented clays on ceramic plates were analyzed by XRD after Mg saturation, liquid glycerol solvation and K saturation (room temperature, heating at 400ºC and 550ºC for 1 h). In order to resolve kaolinite and chlorite peaks for group 3 clays, oxalate-extracted, dry clay samples were ground with 20% of urea (in weight) as described by Gardolinski *et al*. (2001).

Random powder samples of the finely ground sand fraction from some sites were also analyzed by XRD. All XRD patterns were obtained using monochromated CuKα radiation and were interpreted according to Brindley and Brown (1980) and Nriagu and Moore (1984).

Differential thermal and thermogravimetric analyses

Simultaneous differential thermal and thermogravimetric (DTA and TG) analyses of the oxalate-treated

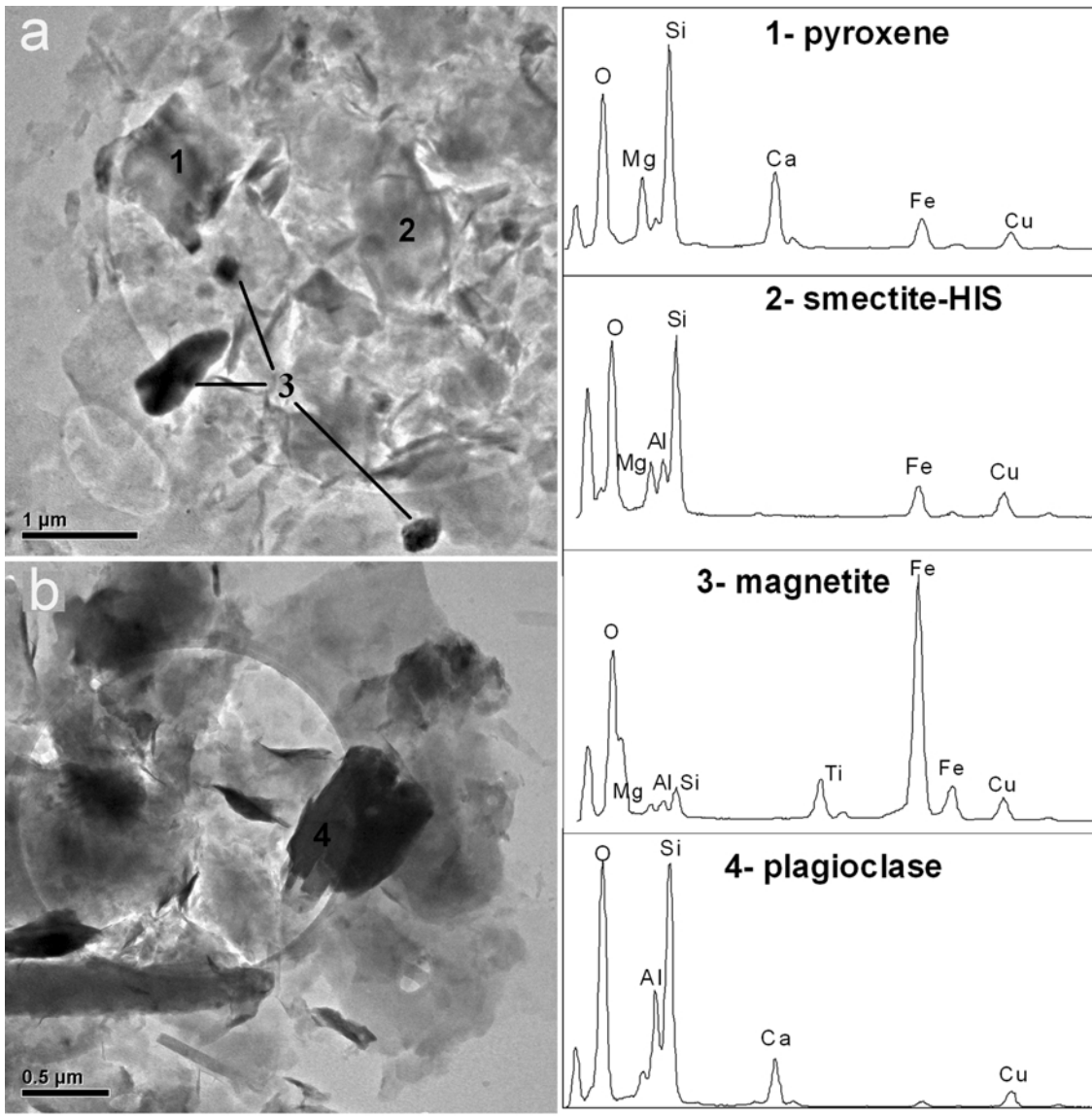

Figure 2. TEM images and qualitative EDS analyses of the clay fraction from site 1. (a) 1 – pyroxene; 2 – interstratified smectite-HIS; 3 – magnetite; and (b) 4 – plagioclase. Cu peaks in the EDS spectra are due to interference from the Cu grid.

samples were carried out using a Shimadzu DTG-60 instrument by heating 20 mg of sample from ambient temperature to 1000ºC at 10ºC min^{-1}, under N_2 atmosphere. In this paper, only data from group 3 sites are presented. Using the TG results, the amount of kaolinite in clay samples from sites 8 and 9 was estimated according to Jackson (1979) and Tan *et al*. (1986).

Transmission electron microscopy and energy dispersive spectrometry

Dilute clay suspensions were mounted on carbon-coated copper grids and analyzed using a JEOL 3000F field emission gun transmission electron microscope (FEG-TEM) equipped with an Oxford Instruments INCA 200 EDS system. All images, EDS analyses and electron diffraction patterns were acquired at 300 kV accelerating voltage.

RESULTS AND DISCUSSION

Group 1 – Basaltic ahumic soils (sites 1 and 2)

The XRD results indicate that the sand fraction (data not shown) of these soils consists mainly of plagioclase (major reflections at 3.21, 3.19 and 2.16 Å), with minor amounts of pyroxene (3.12 and 2.88 Å), magnetite (2.53, 2.44, 2.10 and 1.61 Å) and traces of quartz (3.33 Å). A weak peak at 15.0 Å indicates the presence of smectite in the sand fraction. Plagioclase, quartz, pyroxene and magnetite are also common in the clay fraction as confirmed by TEM/EDS analyses (Figure 2).

Smectites are indicated in the XRD patterns for both sites by the sharp peak at 14.3–14.5 Å for the Mg-saturated sample (Figure 3), expanding to 16.5–16.6 Å after glycerol solvation (Figure 4a,c). The 060 reflection at 1.50 Å (not shown) indicates the dioctahedral nature of this clay mineral (Borchardt, 1989; Egli *et al*., 2001).

For site 1, the K-saturated sample had a peak at 12.7 Å, shifting after heating at 550ºC to a broad peak with two maxima at 12.3 Å and 10.5 Å (Figure 4a). For site 2 a broad asymmetrical peak with maxima at 13.9 Å and 12.4 Å was formed after K saturation, shifting after heating to an asymmetrical peak at 10.3 Å with a broadening towards greater *d* values.

The resistance of the K-saturated mineral to collapse to 10.0 Å even after heating at 550ºC suggests the presence of hydroxy-Al interlayers (Barnhisel and

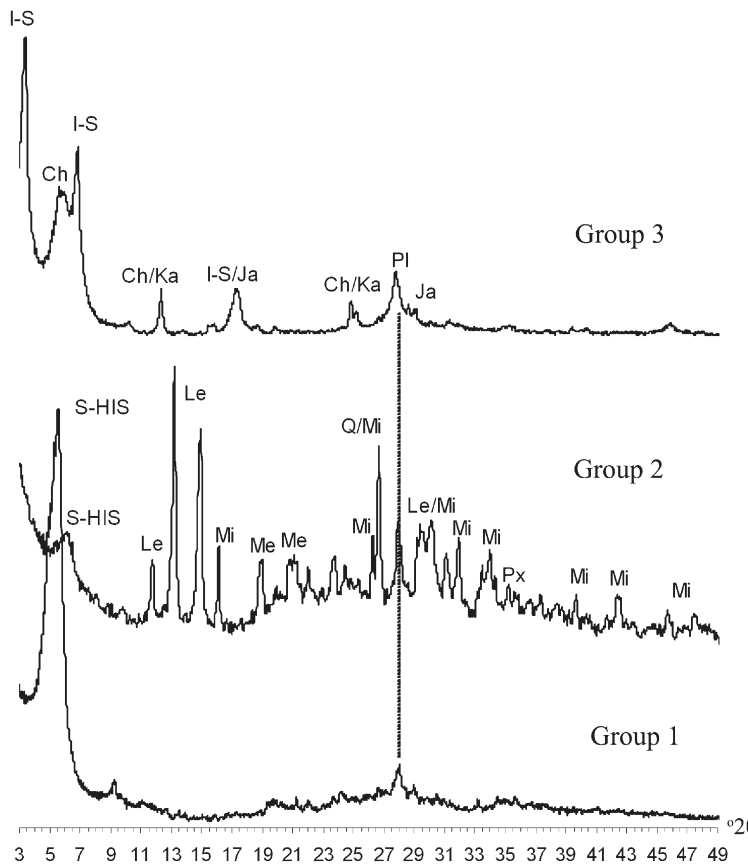

Figure 3. Representative XRD patterns of basally oriented Mg-saturated clays from each soil group. (I-S – interstratified illite-smectite; Ch – chlorite; Ka – kaolinite; Ja – jarosite; S-HIS – interstratified smectite-hydroxy-Al smectite; Le – leucophosphite; Mi – minyulite; Me – metavariscite; Pl – plagioclase; Q – quartz; Px – pyroxene).

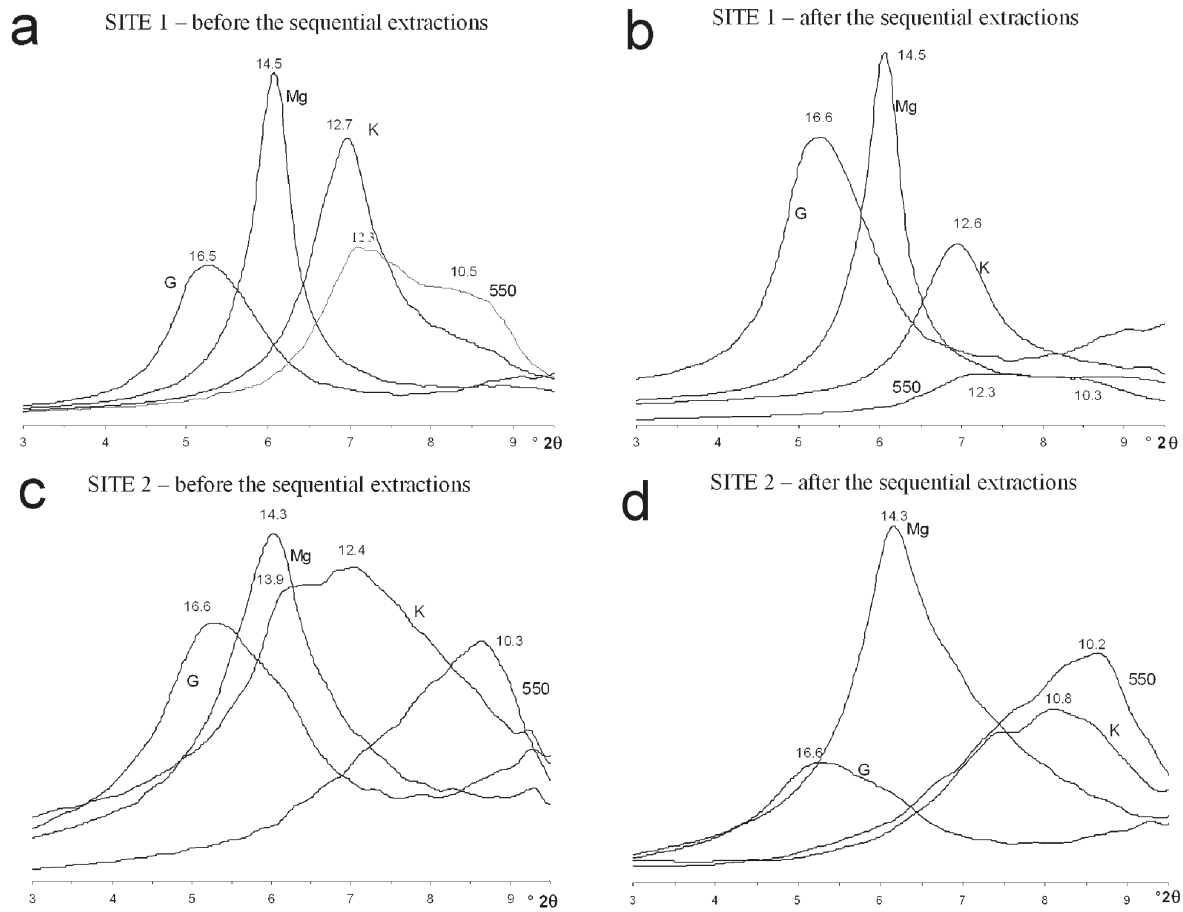

Figure 4. XRD patterns of oriented clay before (a, c) and after (b, d,) the sequential pyrophosphate-oxalate-NaOH extractions showing shifts of the 001 reflection (Å) of the S-HIS mineral for Sites 1 and 2 after the following treatments: G – glycerol solvation; Mg – saturation with $MgCl_2$; K – saturation with KCl at room temperature; 550 – heating at 550 ºC of K-saturated clay.

Bertsch, 1989), characterizing a randomly interstratified smectite-hydroxy-Al smectite (S-HIS). The peak positions after K saturation or glycerol solvation depend on the proportion of each phase in the interstratified mineral (Sawhney, 1989). Greater proportions of HIS layers result in peaks closer to 14.4 Å. Therefore, the results suggest relatively larger proportions of HIS layers for site 2 as the mineral retained a 13.9 Å *d* value after K saturation.

It is also known that more stable interlayer constituents require greater temperatures to produce shifts to lower *d* values for K-saturated clays (Barnhisel and Bertsch, 1989). In the present study, the interlayer component in clays from site 2 was more easily removed by heating and by chemical extractions than for site 1 (Figure 4c,d). The lower stability of the hydroxy-Al component and/or lower degree of interlayer filling for site 2 is suggested by the smaller *d* value obtained after heating at 550ºC in relation to site 1 (Figure 4a,c). For the extracted sample (Figure 4d), a broad peak with a clear maximum at 10.8 Å was formed after K saturation, shifting to 10.2 Å after heating. This indicates that most of the hydroxy-Al interlayers were effectively removed by the sequential extraction. On the other hand, the chemical extractions had little effect on the site 1 sample, indicating the greater stability of the interlayer components.

We found no evidence of neoformation of smectites in soils from Admiralty Bay. The presence of clay-sized pyroxene and plagioclase indicates a very small degree of chemical alteration of the parent material. Jeong and Yoon (2001) and Yong *et al*. (2004) suggested that smectites in King George Island soils are likely to have been inherited from hydrothermal alteration of bedrock. The presence of smectite in the sand fraction of group 1 soils also indicates that the clay fraction may be at least partially inherited through cryoclastic weathering of coarser soil particles.

In the soil environment, the polymerization of hydroxy-Al in the interlayer spaces of smectites is expected even under weak weathering conditions (Borchardt, 1989). The acid attack of both tetrahedral and octahedral sheets of the expansible mineral and the weathering of aluminous minerals such as plagioclases are possible sources of hydroxy-Al polymers (Wilson, 1999).

Approximately 25 (±0.4)% of the clay fraction was removed by chemical extractions for site 1 and 14 (±1.4)% for site 2 (*i.e.* total mass removal − Table 3). As the Na pyrophosphate and ammonium oxalate extractions are assumed to have had no effect on crystalline minerals, the total mass removal (TMR) by

Table 3. Sequential extraction data for the clay samples.

Depth	Pyrophosphate			NH_4 oxalate				NaOH[1]			Mass removal[2]				
	Al_2O_3	Fe_2O_3	SiO_2	Al_2O_3	Fe_2O_3	SiO_2	P_2O_5	Al_2O_3	SiO_2	P_2O_5	TMR	Pyr	Ox	NaOH	Pyr+Ox
cm	(g/kg)										(%)				
Site 1															
0−10	5.2	1.0	0.0	31.8	7.7	30.2	7.2	11.6	6.2	0.8	24.9	3.6	12.1	9.2	15.7
10−20	5.5	0.7	0.2	27.0	7.1	34.2	6.8	6.3	5.2	0.5	24.3	3.7	13.1	7.5	16.8
Site 2															
0−10	3.5	2.2	3.7	9.4	6.9	11.2	6.8	3.9	3.5	0.4	20.6	2.6	5.7	7.9	8.3
10−20	2.1	1.9	1.7	10.5	6.7	14.0	5.9	3.3	3.1	0.4	18.7	2.7	5.4	5.9	8.1
20−30	1.5	0.7	1.0	10.1	6.0	15.6	5.9	3.4	3.2	0.5	23.5	0.4	5.4	7.1	5.8
30−40	1.8	1.4	1.2	9.9	6.6	11.5	5.7	2.6	2.7	0.5	23.7	1.1	7.5	7.1	8.7
40−50	2.0	1.3	2.2	8.7	5.6	11.4	4.9	2.9	2.6	0.6	26.3	1.6	4.6	7.0	6.2
50−60	1.7	0.9	1.7	10.2	6.2	13.3	5.6	3.3	2.7	0.4	20.6	0.6	5.9	7.2	6.5
Site 3															
10−20	40.3	24.7	3.5	25.2	18.7	13.0	43.4	3.8	5.5	0.4	48.1	27.7	10.7	9.7	38.4
20−30	38.6	22.6	5.3	29.0	38.4	9.3	69.3	2.9	4.8	0.3	52.7	27.2	17.2	8.3	44.4
30−40	24.2	17.2	3.2	35.1	41.7	8.4	74.7	5.4	5.6	1.1	53.3	17.9	23.6	11.8	41.5
40−50	24.5	21.8	3.9	31.7	24.4	6.7	53.2	19.7	13.7	28.9	60.0	16.1	19.2	24.7	35.3
Site 4															
0−10	30.7	20.7	1.5	16.1	11.3	7.6	9.6	8.4	13.3	5.4	44.2	21.0	7.4	15.8	28.4
10−20	52.2	41.3	2.5	26.8	14.9	9.4	20.5	12.1	19.7	4.7	67.1	39.5	10.1	17.5	49.6
20−30	78.4	28.8	5.0	33.1	15.6	5.7	31.7	71.0	8.6	102.0	82.8	46.2	11.7	24.8	57.9
30−40	65.7	18.2	1.7	30.3	14.1	4.3	33.2	94.5	7.9	135.1	81.6	32.2	12.9	36.6	45.1
40−50	58.0	21.9	2.3	29.2	15.4	7.7	28.3	62.0	17.3	87.5	70.3	29.0	13.6	27.6	42.6
50−60	58.1	20.9	2.1	30.7	16.5	4.6	32.4	81.6	13.1	112.3	78.0	27.7	13.7	36.6	41.4
60−70	66.1	26.8	5.8	36.4	17.1	5.6	36.6	80.1	14.4	111.9	81.6	37.8	13.9	30.0	51.7
Site 5															
0−10	20.9	15.2	2.1	16.6	11.0	11.7	5.7	5.2	9.7	0.7	38.0	20.6	7.9	9.5	28.5
10−20	25.1	22.0	1.4	16.4	13.6	9.2	7.3	6.0	9.8	1.1	38.6	18.7	8.7	11.2	27.4
20−30	26.1	29.1	6.2	13.2	16.6	5.9	8.8	6.5	8.8	1.6	38.3	23.5	7.0	7.8	30.5
30−40	32.0	35.2	10.9	13.2	15.7	5.7	8.2	7.1	8.3	1.0	36.5	23.7	7.0	5.8	30.7
40−50	38.5	33.0	11.3	13.6	15.5	5.7	9.1	6.1	8.1	1.0	42.9	26.3	8.8	7.7	35.2
Site 6															
10−20	18.5	20.8	4.0	12.9	9.6	7.6	15.1	3.7	8.8	1.4	62.8	26.2	21.2	15.3	47.4
20−30	23.6	26.5	2.5	19.3	15.3	9.0	18.6	4.0	10.2	0.8	46.9	24.6	9.5	12.8	34.1
30−40	36.4	39.8	3.9	16.3	12.5	8.5	13.9	4.0	10.3	0.9	52.7	31.7	8.0	13.0	39.7
Site 7															
10−20	26.4	28.7	1.8	12.2	10.0	8.1	10.5	4.3	9.0	1.4	51.5	30.2	7.1	14.3	37.3
20−30	16.8	22.9	1.4	10.8	9.1	5.7	10.5	3.8	8.6	1.2	51.0	31.5	6.4	13.0	38.0
30−40	88.3	61.5	2.0	10.5	6.8	6.2	6.6	3.5	8.6	1.2	67.7	52.8	4.0	11.0	56.7
40−50	38.5	28.9	2.0	13.9	14.0	7.1	15.7	3.9	5.9	3.2	59.5	41.7	6.5	11.3	48.2
Site 8															
0−10	1.9	0.6	0.0	2.8	6.0	0.5	1.0	3.0	8.2	0.4	14.7	8.7	3.7	2.3	12.4
10−20	5.3	1.4	1.9	3.1	15.8	0.6	4.3	2.1	6.7	1.1	21.3	14.1	5.0	2.2	19.1
20−30	7.0	1.6	3.9	2.9	14.1	0.6	3.7	1.6	5.8	0.7	22.8	13.7	6.0	3.2	19.6
Site 9															
0−10	6.8	2.0	6.8	7.3	15.7	4.5	5.6	3.9	1.5	0.9	20.1	3.5	8.2	8.5	11.7
10−20	5.0	1.5	4.7	6.9	20.5	3.9	6.0	3.3	1.3	1.0	21.1	1.9	8.5	10.7	10.4
20−30	22.8	6.3	26.9	4.2	21.3	2.0	8.2	3.0	1.5	1.1	26.0	7.2	9.3	9.5	16.5
30−40	26.5	7.2	32.8	3.9	22.0	1.8	8.4	2.5	1.3	1.1	27.4	8.5	9.3	9.6	17.8
40−50	11.0	4.2	10.8	4.7	23.4	1.3	5.8	3.2	1.4	1.0	21.8	6.1	6.5	9.2	12.6
50−60	14.9	4.4	15.1	3.8	21.2	1.9	5.4	3.6	1.5	1.1	24.6	10.1	5.8	8.7	15.9

[1] The Fe_2O_3 levels in the NaOH extracts are < detection limit and therefore are not presented
[2] % of mass removal from the clay fraction by each extractant: TMR − total mass removed
Pyr = Na pyrophosphate extraction; Ox = NH_4 oxalate extraction

Table 4. Mean values and standard errors ( ) of Al/Si and $P_2O_5/(Al_2O_3 + Fe_2O_3)$ ratios for oxalate extracts of the clay fractions.

Depth (cm)	Alo/Sio	$P_2O_5/(Al_2O_3 + Fe_2O_3)$
Site 1		
0–20	0.9 (0.1)	0.2 (0.0)
Site 2		
0–60	2.0 (0.4)	0.4 (0.0)
Site 3		
10–20	1.9	1.0
20–50	4.0 (0.8)	1.0 (0.1)
Site 4		
0–20	2.5 (0.4)	0.4 (0.1)
20–70	6.0 (1.3)	0.7 (0.0)
Site 5		
0–50	2.0 (0.4)	0.3 (0.0)
Site 6		
10–40	1.9 (0.2)	0.6 (0.1)
Site 7		
10–50	1.8 (0.2)	0.5 (0.1)
Site 8		
0–10	5.1	0.1
10–30	5.3 (0.3)	0.2 (0.0)
Site 9		
0–60	2.2 (0.7)	0.3 (0.1)

these extractions provides an estimate of the non-crystalline components in the clay fraction. For sites 1 and 2, the non-crystalline phases account for 16 (±0.8)% and 8 (±1.2)% of the clay fraction, respectively (Table 3). The oxalate extraction accounted for 80% of these amounts, indicating that X-ray amorphous allophane-like minerals were the main extracted phases.

The DXRD patterns obtained after the oxalate extraction (pyr-ox) resemble those described for allophane, with broad maxima at 3.3 and 2.2 Å (Campbell and Schwertmann, 1985; Wada, 1989; Parfitt, 1990). The Al/Si ratio in the oxalate extracts for both sites is close to 1.0 (Table 4), which is similar to Si-rich allophanic materials described by Parfitt (1990). Pumice allophane (Farmer *et al*., 1979), defect kaolin allophane (Parfitt and Wilson, 1985) and halloysite-like allophane (Yoshinaga, 1986) are names which have been proposed for Si-rich allophanes (Parfitt, 1990). The amount of amorphous allophane-like phases is obtained by multiplying the % Si in the oxalate extract by 5 (Parfitt, 1990; Smith, 1994). Approximately 14% and 6% of the clay from sites 1 and 2, respectively, is composed of a Si-rich allophane-like phase(s).

Group 2 – ornithogenic soils (sites 3–7)

Similarly to group 1 soils, the interstratified S-HIS is the dominant crystalline clay mineral in the clay fraction of group 2 soils (Figure 3). Similar peaks before and after the chemical extractions for all clay treatments suggest that little of the interlayer component was removed. All group 2 soils also contain small amounts of quartz, plagioclase and Fe-Ti oxides in the clay fraction as confirmed by TEM/EDS analysis (Figure 5). Apart from this similarity in clay mineralogy, the XRD patterns indicate that there are pronounced mineralogical differences from group 1 soils for those sites directly (3 and 4) or indirectly (5, 6 and 7) influenced by penguin activity. For the former sites, sharp, intense peaks of several crystalline phosphates occur which are listed in Table 5 and illustrated in Figure 3. These minerals were present only in layers deeper than 20 cm at both sites (3 and 4).

The sequential extractions removed, on average, 53.5 (±4.9)% and 72.3 (±13.8)% of the clay fraction for sites 3 and 4, respectively (Table 3 – TMR). Similarly to group 1, the amount of non-crystalline phases (bound organic matter and X-ray amorphous Al, Fe, Si-P minerals) was estimated from the mass removed by the pyr and ox extractions (Table 3).

The DXRD (pyr-ox) patterns of group 2 clays present broad lines with maxima at 3.3 and 2.2 Å indicating the removal of X-ray amorphous minerals. The NaOH extraction resulted in the complete dissolution of crystalline phosphates for all samples from site 4 (Figure 6) and for the deepest layer of site 3 (not shown). For the upper layers of site 3, a crystalline phosphate with similar *d* values to leucophosphite persisted after the NaOH extraction (Figure 7). For samples from which all crystalline phosphates were dissolved, the mass removal by the NaOH extraction gives an estimate of the amount of these minerals (Table 3 – site 3 and deepest layer of site 4).

For site 3, 41.4 (±3.9)% of the clay fraction was removed by the pyr + ox extractions (non-crystalline phases). For site 4, these phases account for 45.2 (±9.4)% of the clay fraction. Approximately 73.2% (site 3) and 55.6% (site 4) of the non-crystalline components were removed by the pyrophosphate

Table 5. Crystalline phosphates identified in the clay fraction for sites 2 and 3.

Name	Chemical formula	Main XRD peaks (Å)
Leucophosphite	$K_2(Fe^{3+},Al)_4(PO_4)_4(OH)_2.2H_2O$	7.63, 6.79, 5.99, 3.061
Minyulite	$KAl_2(PO_4)_2(OH,F).4H_2O$	6.8, 5.6, 3.38, 3.07, 2.61, 2.38, 2.14
Metavariscite	$Al(PO_4).2H_2O$	2.77, 4.33, 4.67

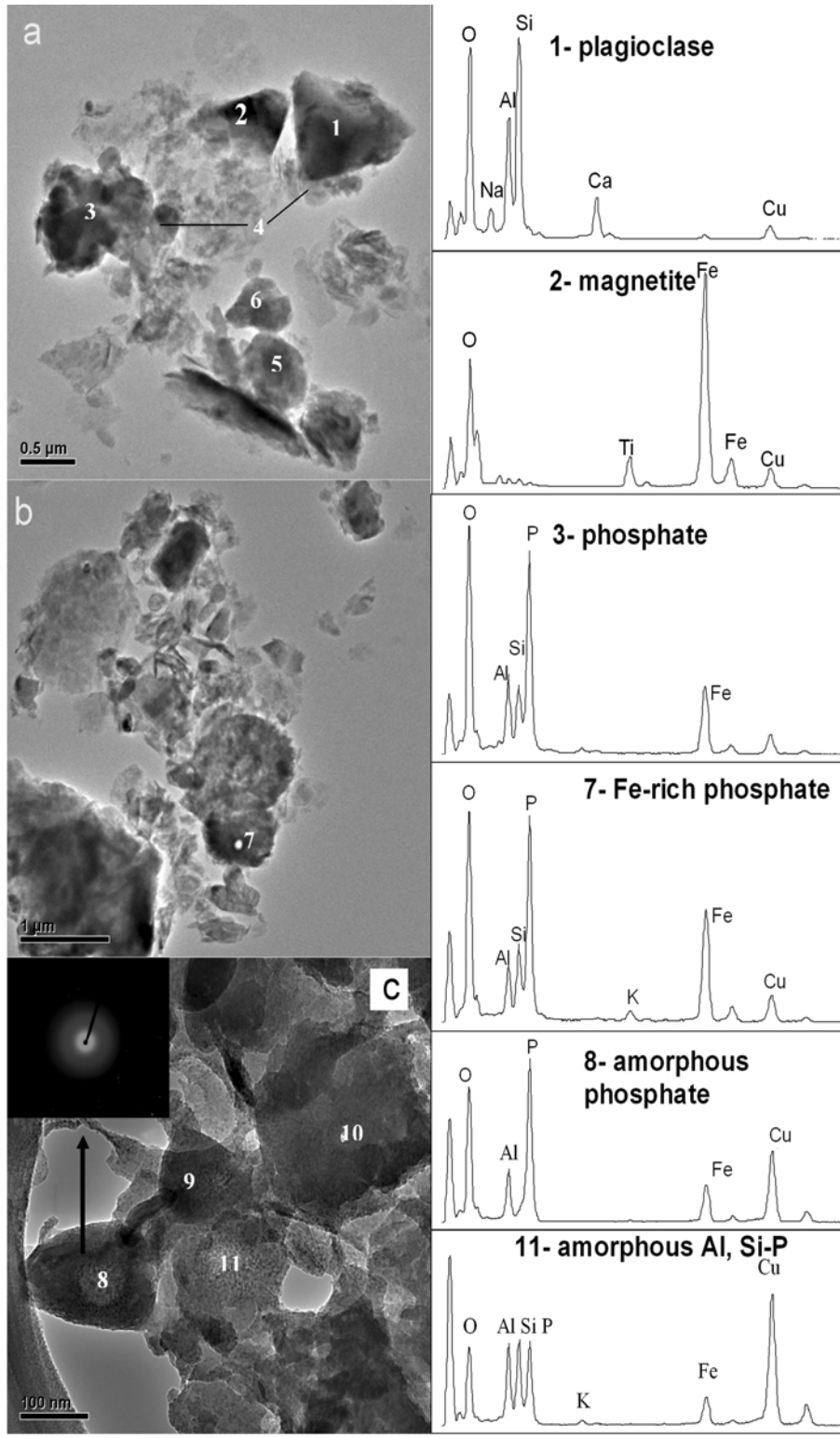

Figure 5. TEM images, qualitative EDS analysis and electron diffraction of the clay fraction from site 3. (a) 1: plagioclase fragment; 2: Ti-rich magnetite; 3–5: Al-Fe phosphates; 6: pyroxene. (b) Fe phosphate in clay from site 3 after the sequential extractions (Fe-P). (c) 7–9: X-ray amorphous Al and Fe phosphates; 10–11: X-ray amorphous Al, Si and P phase. All features from c yielded electron diffraction patterns typical of X-ray amorphous materials (broad rings) as illustrated for C-8. Cu peaks in the EDS spectra are due to the Cu grid.

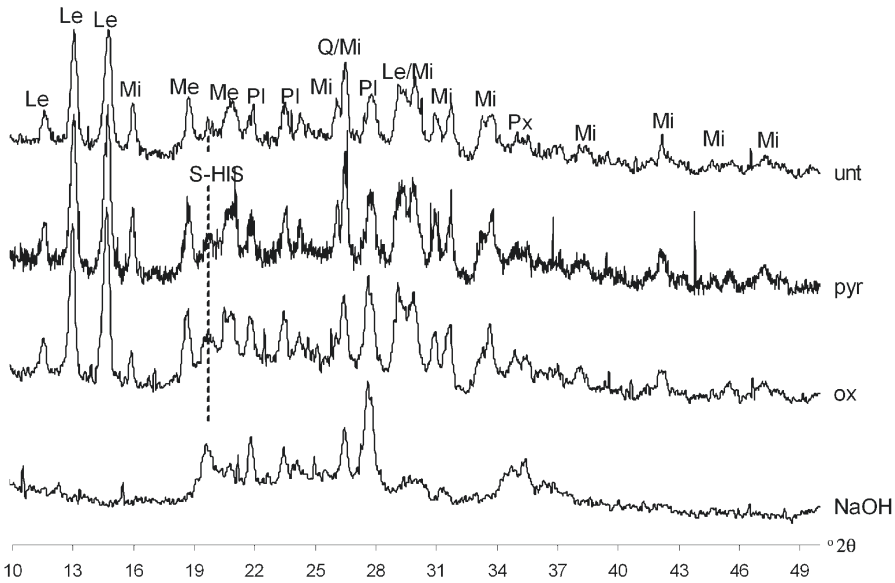

Figure 6. Random powder XRD patterns of the clay fraction from a phosphatic layer of site 4 after each chemical extraction. Le – leucophosphite; Me – metavariscite; Mi – minyulite; S-HIS – interstratified smectite-hydroxy-Al smectite; Pl – plagioclase; Q – quartz; Px – pyroxene; unt – untreated sample; pyr – after pyrophosphate extraction; ox – after pyr + oxalate extraction; NaOH – after pyr + ox + NaOH extractions.

extraction, demonstrating the significant participation of phases bound to organic matter (Table 3). This was expected due to the large organic C content in these sites compared to groups 1 and 3. At the deepest layer of site 3, 24.7% of the clay fraction was removed by the NaOH extraction (crystalline phosphates) and for site 4, an average of 31.1 (±5.3)% of the clay below 20 cm deep is composed of these minerals (Table 3).

For sites 3 and 4 (Table 3), the oxalate extracts had the highest P levels of all sites (site 2 – 72.0±3.8 g/kg and site 3 – 32.4±3.0 g/kg) with the $P_2O_5/(Al_2O_3 + Fe_2O_3)$ ratio ranging from 0.7 to 1.0 and with extremely high values for the Al/Si ratio (Table 4). This suggests that X-ray amorphous Al and Fe phosphates were the main extracted phases. The TEM/EDS analysis confirmed the abundance of spherical phosphate aggregates containing various amounts of Al, Fe and K (Figure 7). For the 20–40 cm layer of site 3, P and Fe levels in the oxalate extracts were greater than for any of the other studied sites, with Fe exceeding Al (Table 3). On the other hand, for all layers of site 4, Al levels are nearly twice as great as those of Fe in the oxalate extract (Table 3).

As described in detail by Polish researchers, various processes are responsible for the paragenesis of phosphates in ornithogenic soils of Maritime Antarctica (Tatur and Myrcha, 1993; Myrcha *et al*., 1985; Tatur and Barckzuc, 1985). Continuous manuring and the availability of large amounts of liquid water promote percolation of alkaline solutions which lead to the formation and persistence of phosphates. After site abandonment by penguins, soil acidification and percolation of alkali-poor rain or melt water cause the alteration and dissolution of these minerals, leading to the formation of X-ray amorphous Fe, Al-P phases.

Sites 3 and 4 are abandoned rookeries where exuberant vegetation has developed (Tatur *et al*., 1997; Simas *et al*., 2005). Struvite and hydroxylapatite, typical of surface guano layers in active rookeries (Tatur and Myrcha, 1993), are no longer present due to their lack of stability in the current pedoenvironmental conditions. Nevertheless, even after a long period of abandonment, Al and Fe phosphates constitute the main crystalline components of the clay fraction for these sites, thus constituting a long-term reserve of P for plant nutrition. Previous work suggests that some of these rookeries are >500 y old (Tatur *et al*., 1997).

The higher Fe levels in the oxalate extracts (Table 3) and the XRD patterns (Figure 6) suggest that the crystalline P mineral in the clay from the 20–40 cm layers of site 4 is Fe-rich leucophosphite. The TEM/EDS analyses revealed the presence of Fe-rich phosphates in a sample from site 4 previously extracted with NaOH, supporting this interpretation (Figure 7). This might explain the ineffectiveness of the NaOH extractant in removing the crystalline phosphates from these layers. Due to the insolubility of Fe at high pH (Smith, 1994), the NaOH extraction is not efficient in removing crystalline Fe-P minerals (Table 3, Figure 7).

Samples from sites 5, 6 and 7 do not contain crystalline phosphates. The TMR by the sequential extraction for each site was 38.9 (±2.4)%, 57.4 (±7.9)% and 54.1 (±8.0)%, respectively (Table 3). For these sites, because little hydroxy-Al interlayer component and no crystalline minerals were removed, the TMR

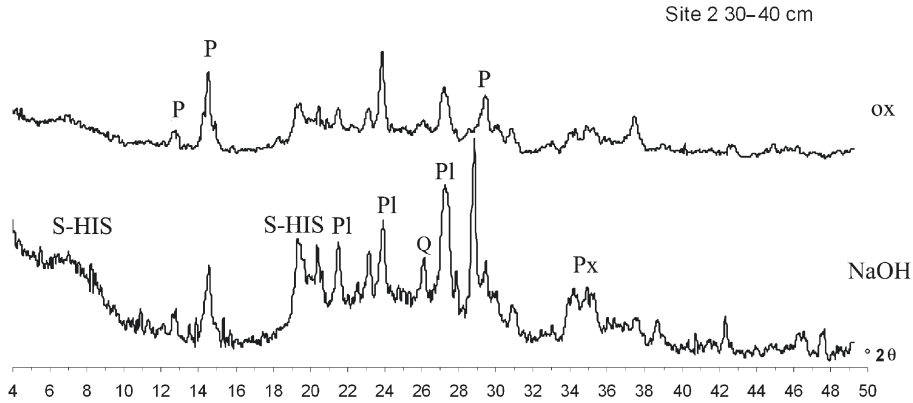

Figure 7. Random powder XRD patterns of the clay fraction from site 3 after oxalate (ox) and oxalate + NaOH (NaOH) extractions. An unidentified crystalline phosphate (P) yielding peaks similar to those of leucophosphite persisted after the NaOH extraction for the 30−40 cm layer while for the deepest layer (40−50 cm) there was complete removal of crystalline phosphates (not shown). S-HIS − hydroxy-interlayered smectite; Pl − plagioclase; Q − quartz; Px − pyroxene.

values give an idea of the amount of non-crystalline phases in the clay fraction from these sites. Similarly to sites 3 and 4, pyrophosphate-extractable phases account for ~60% of the TMR, with increasing levels of Al, Si and Fe with depth (Table 3). For site 6, a buried O horizon (30−40 cm layer) favors the accumulation of Al and Fe bound to organic matter. The oxalate extract had a mean Al/Si ratio of 2.0 and relatively low P levels (7.8−15 g/kg), with the $P_2O_5/(Al_2O_3 + Fe_2O_3)$ ratio ranging from 0.3−0.6 (Table 4). NaOH extracted very little P and the Al/Si ratio <0.9 for this extractant indicates the removal of an X-ray amorphous Si-rich phase(s) (Table 3).

The composition of the oxalate extracts suggests that much P is adsorbed onto allophane-like phases for sites 5, 6 and 7. Due to the high organic C content (Table 2), some of the P is also likely to be adsorbed by humus-Al complexes. Allophane-like minerals, ferrihydrite and Al-humus complexes are the most likely to react with P in acid soils (Parfitt and Kimble, 1989). P-allophane reactions start with rapid strong adsorption followed by a slower, weaker adsorption. As the P concentration increases the disruption of the allophane structure, precipitation of crystalline or/and non-crystalline Al phosphates occurs. Even in soils where allophane is not present, Al phosphates can precipitate from reactions with Al-humus species if high levels of phosphate are present (Parfitt and Kimble, 1989). Similarly, reactions with X-ray amorphous Fe oxides can lead to the formation of Fe phosphates in acid (pH 2.3−4.9) pedoenvironments.

Amorphous Si-rich particles resembling grass opal phytoliths (Drees *et al*., 1989) are also common in the clay fraction for all ornithogenic sites but were not present in groups 1 and 3 soils (Figure 8). This is consistent with the development of exuberant *Deschampsia Antarctica* (gramineae) communities at ornithogenic sites.

Group 3 − acid sulfate soils (sites 8 and 9)

Quartz and plagioclase are the main minerals in the sand fraction of these soils. Chlorite is also present with an intense peak at 7.06 Å and a much weaker peak at 14.2 Å, corresponding to the 002 and 001 reflections. For the clay fraction, peaks at 24.4 Å, 12.07 Å and 8.1 Å after Mg saturation correspond to the 001, 002 and 003 reflections, respectively, of a regularly interstratified clay mineral composed of 10 Å and 14 Å layers (Figure 3). After glycerol solvation the 001 peak expanded to 27.6, with higher-order reflections at 13.8 (002) and 9.4 Å (003), suggesting the presence of smectite layers (not shown). After K saturation, a peak at 21.5 Å was formed and heating to 550ºC yielded a 21.0 Å peak. These results suggest that the mineral is a regularly interstratified illite-smectite (I-S). Chlorite is also present in the clay fraction as shown by the 14.8 Å (001), 7.12 Å (002), 4.99 Å (003) and 3.54 Å (004) peaks, all unaffected by glycerol or K saturation. A peak at 1.50 Å (060 reflection) and no peak at 1.54 Å suggest a dioctahedral structure for the illite-smectite and possibly the chlorite (not shown) (Egli *et al*., 2001).

The XRD patterns of oxalate-extracted samples have peaks at 3.57 Å (kaolinite 002 peak) and 3.54 Å (chlorite 004 peak) (Figure 9a). After the urea treatment, part of the 7.12 Å peak shifted to 7.6−7.8 Å, indicating the increase of kaolinite d_{001} values due to the penetration of urea into interlamellar spaces of kaolinite (Gardolinski *et al*., 2001) (Figure 9b). The remaining 7.12 Å peak indicates the presence of chlorite, which was unaffected by the urea treatment. Results from DTA analysis (not shown) also support the presence of kaolinite with the main endothermic peak occurring between 460 and 490ºC while an incipient exothermic peak occurred between 950 and 1000ºC. Chlorite endothermic (600ºC) and exothermic (850−900ºC) peaks are also present. Based on TG data, the estimated total amounts of kaolinite in the clay fraction were 22.2

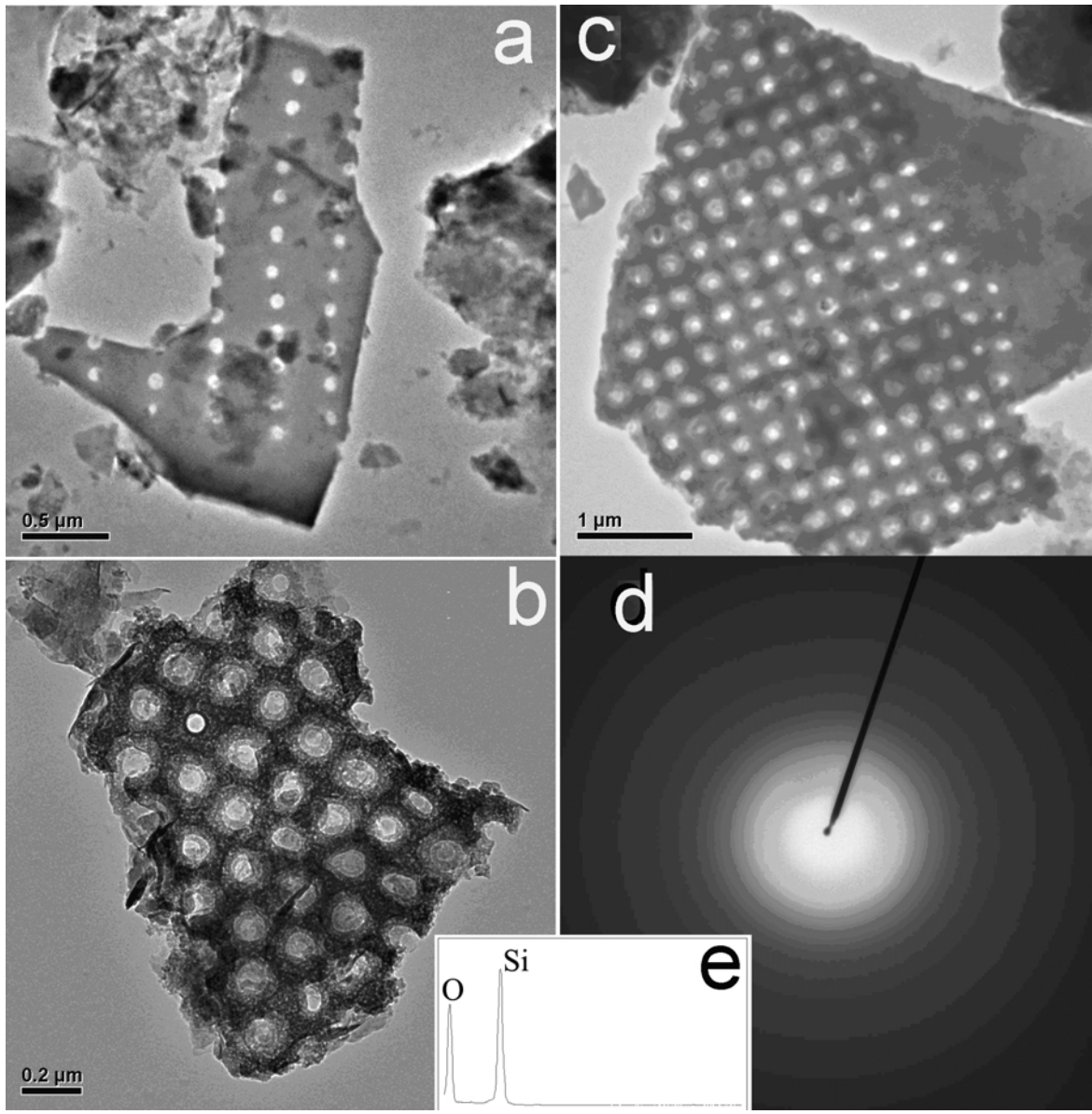

Figure 8. X-ray amorphous Si bodies (a–c) in the clay fraction of ornithogenic soils, resembling grass root opal (Drees *et al.*, 1989). All particles showed similar Si, O chemical composition (e) and electron diffraction patterns of X-ray amorphous silica (d).

(±0.3)% and 40.1 (±2.8)% for sites 8 and 9, respectively. The TEM/EDS analyses confirmed the presence of kaolinite and indicate that it occurs mainly as rather asymmetrical plates and very rarely as typical hexagonal crystals (Figure 10a,c). The electron diffraction patterns of the kaolinite crystals consist of a hexagonal *hk* network based on b = 9.0 Å.

The plagioclase content in the clay fraction is negligible with no characteristic sharp peaks at 3.19 and 3.20 Å. Jarosite was identified by the 5.09 (012), 3.08 (113) and 3.11 Å (021) reflections for site 9 (Figure 11), although they were absent for site 8. The TEM/EDS analyses confirm the abundance of jarosite crystals in the clay fraction of site 9 (Figure 10b). Various amounts of K and Na in the different jarosite crystals indicate that jarosite is commonly intermediate to natrojarosite.

Interstratified I-S, chlorite and kaolinite have been described previously for soils on King George Island and were attributed to paleohydrothemal alteration of mica-bearing granodiorites (Yong *et al*., 2004). Wilson (1999) considers it unlikely that I-S forms as a stable phase in soils due to the elevated temperature and pressures needed for its formation in diagenetic sequences. However, Bergkraut *et al*. (1994) have described regularly interstratified I-S formed under Earth-surface

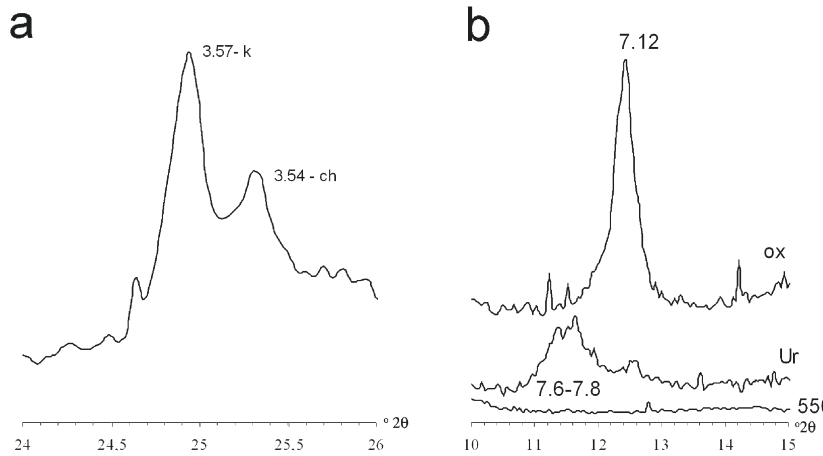

Figure 9. XRD patterns of the clay fraction from site 9 after pyrophosphate and oxalate extractions indicating the presence of both chlorite and kaolinite; 9a shows distinguishable peaks at 3.57 Å for kaolinite and 3.54 Å for chlorite. 9b shows the expansion of the kaolinite 001 peak to 7.6–7.8 Å after urea treatment, with no effect on the chlorite 002 peak.

conditions due to weathering of basic pyroclastics. Środoń and Eberl (1984) also present evidence of illitization under pedogenic temperatures due to wetting and drying of smectites in the presence of K.

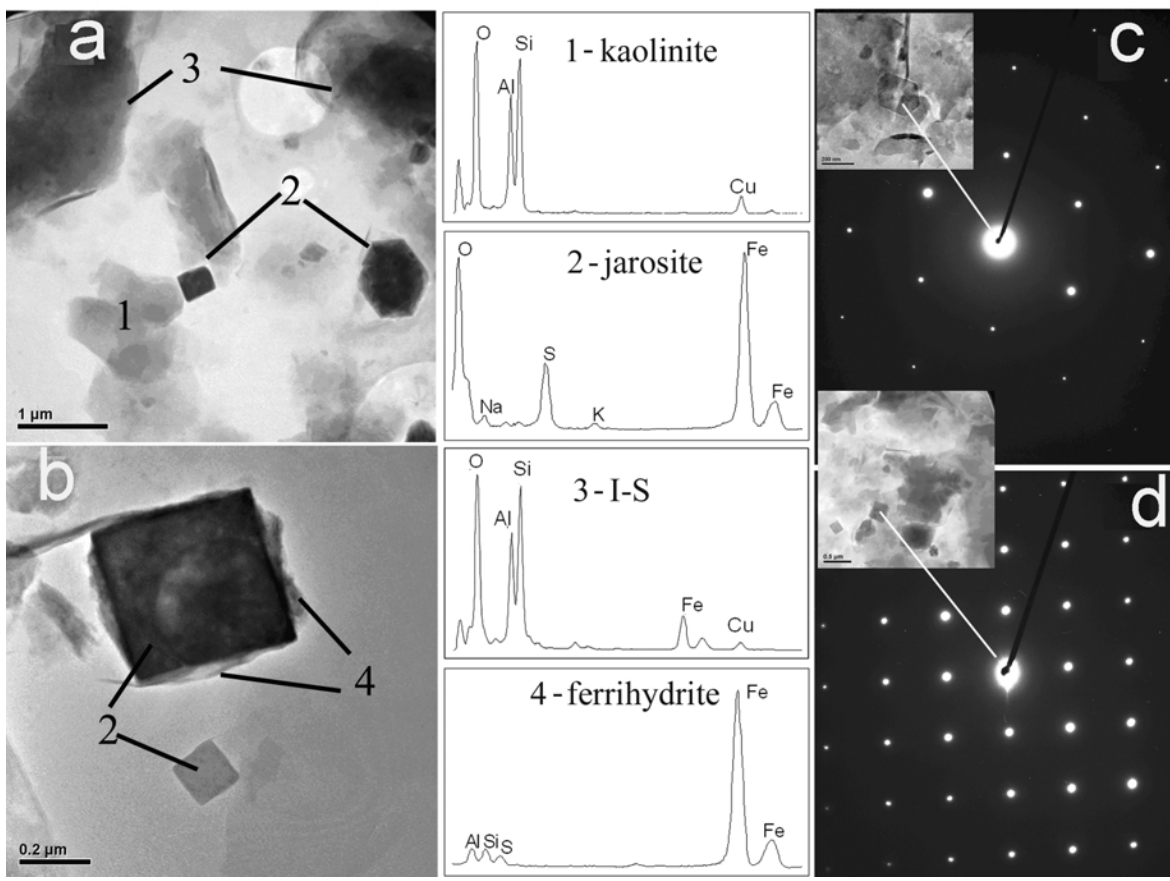

Figure 10. TEM images and EDS of clay from site 9. (a) 1 – subheudral kaolinite plates; 2 – jarosite crystals; 3 – interstratified illite-smectite; (b) 4 – ferrihydrite; (c) electron diffraction pattern (EDP) of a hexagonal kaolinite crystal; and (d) EDP of a single jarosite crystal.

Wetting and drying cycles take place in Cryosols from Maritime Antarctica due to their frequent daily freeze-thaw cycles. Ultra-desiccation of soil constituents due to freezing is an important, well-known process in Cryosols (Ostroumov, 2004; Van Vliet-Lanoë *et al*., 2004). Under such conditions, illitization of smectites may take place. Sea-spray, bird droppings, weathering of plagioclases and transformation of jarosite to X-ray amorphous Fe oxides are possible sources of K.

Oxidation of pyrite has resulted in acid sulfate weathering, with precipitation of jarosite and/or natrojarosite. As outlined by Doner and Lynn (1989), the acidity produced by this transformation has a strong impact on layer silicate stability, particularly for the interlayers of 2:1 silicates, leading to the degradation of chlorites and smectites. The absence of plagioclases in the clay fraction of sites 8 and 9 suggests that chemical weathering is an important process at these sites. Although kaolinite may be inherited from the hydrothermal alteration of parent materials, chemical weathering of plagioclases to clay minerals is also a possible explanation for its presence in acid sulfate soils of Admiralty Bay.

The TMR by the sequential extractions were 22.0 (±1.0)% and 23.5 (±2.9)% for sites 8 and 9, respectively. Based on the mass removal by the pyrophosphate and oxalate extractions, non-crystalline phases account for 19.3 (±0.4)% and 14 (± 3.0)% of the clay fraction for sites 8 and 9, respectively (Table 3). Pyrophosphate accounted for >60% of the total mass removal for site 8, while for site 9 a gradual increase from 10 to 40% occurred with depth (Table 3). For both sites, pyrophosphate-extractable Al, Fe and Si increased with depth with an abrupt increase in the 20−40 cm layers of site 9 (Table 3). Since these soils have negligible organic C contents, X-ray amorphous Al, Fe and Si compounds were probably the main phases extracted with pyrophosphate.

The oxalate extraction accounted for >20% of the TMR in site 8. For site 9, a gradual reduction from 40 to 20% with depth was observed (Table 3). The Fe levels for the oxalate extracts were very high (2−5 times higher than Al), suggesting that X-ray amorphous Fe (ferrihydrite) was the main phase extracted (Table 3). Relatively high P levels (comparable to some ornithogenic sites) suggest that is P adsorbed onto X-ray amorphous Fe minerals (Table 3). Weathering of mafic minerals such as pyroxenes and amphiboles, Fe-chlorite and hydrolization of jarosites are possible sources of X-ray amorphous Fe phases. A close association between X-ray amorphous Fe-rich phases and jarosite crystals was indicated by TEM/EDS analyses (Figure 10).

Boiling NaOH removed <20% of the TMR for site 8 and nearly 50% for the first 20 cm of site 9, with the amount gradually decreasing with depth to 35% (Table 3). Jarosite was the main mineral removed by NaOH for site 9 (Figure 11), with no effect of extraction on crystalline clay minerals. Therefore we can estimate that jarosite accounts for ~8−10% of the clay fraction for this site.

These data suggest that intense acid weathering is occurring with accumulation of X-ray amorphous phases at depth. This is more noticeable for site 9, where larger amounts of pyrophosphate-extractable Al, Si and Fe in the 20−40 cm layers (Table 3) coincide with the mean permafrost depth at this site. Accumulation of X-ray amorphous Fe, Al and Si gels in the permafrost layer is common in Cryosols, being facilitated by the thermally induced water potential starting from the onset of thaw (Van Vliet-Lanoë *et al*., 2004).

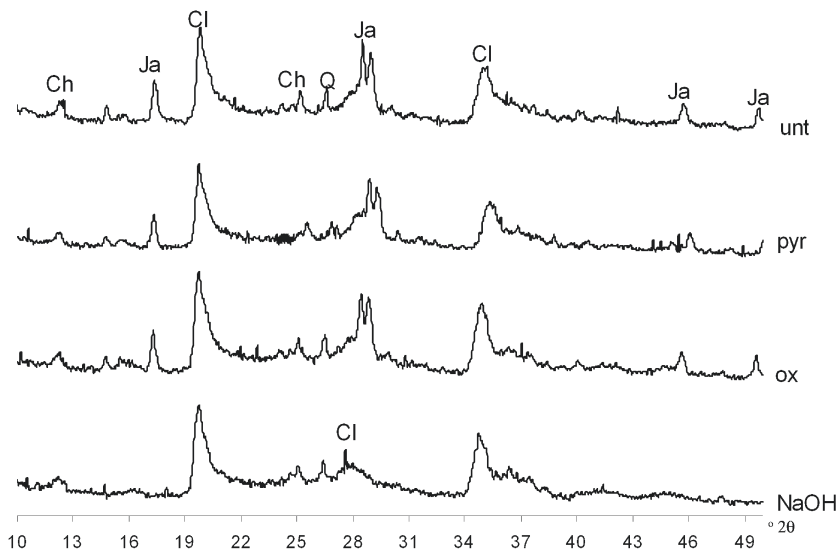

Figure 11. Random powder XRD patterns of the clay fraction from site 9, after each chemical extraction. (Cl − reflections common to all clay minerals, in this case chlorite, I-S and kaolinite; Ja − jarosite; Q − quartz; Ch − chlorite).

CONCLUSIONS

Clay-sized minerals on ahumic basaltic sites of Admiralty Bay are mainly inherited from hydrothermally altered parent materials through physical particle-size reduction promoted by soil freeze-and-thaw cycles. In the soil environment, these materials undergo chemical weathering with formation of interestratified S-HIS and allophane-like phases.

The interaction between penguin guano and inherited clay-sized minerals leads to the formation of crystalline Al and Fe phosphates which constitute long-term P reserves on abandoned rookery sites on basaltic substrates. Leaching of P-rich solutions affects areas adjacent to penguin rookeries reacting with soil organic matter and allophane-like phases. The extremely large proportions of non-crystalline phases indicate that the chemical characteristics of ornithogenic sites are determined by these highly reactive phases. Future monitoring of the chemistry of such phases may be useful in assessing anthropogenic impacts and environmental health.

Soils formed from sulfide-bearing andesites undergo intense acid sulfate weathering with the formation of jarosite and X-ray amorphous Al-Si and Fe minerals. The clay fraction is made up mainly of inherited interstratified I-S and chlorite as well as kaolinite. Intense weathering of primary plagioclases in these soils may lead to the formation of kaolinite.

Contrary to continental Antarctic Cryosols, where physical weathering dominates, chemical weathering is an active process in Cryosols from Admiralty Bay with dissolution of primary alumino-silicates and limited leaching of dissolved Al, Fe and Si. Chemical weathering is enhanced at some sites by the oxidation of sulfides present in the parent material and by faunal activity.

ACKNOWLEDGMENTS

We thank the Brazilian National Research and Technology Council (CNPq) for financing this research and the Brazilian Navy for the logistics during the Antarctic expeditions. Also, we thank the Polish staff at the Henry Arctowski Station during the summers of 2002/2003 and 2004/2005 for their support and, in particular, Prof. Andrej Tatur of the Polish Academy of Sciences for his inspiring observations during field work. The first author thanks Prof. Gilkes and the staff of the Soil Science Department at the University of Western Australia (UWA) for the time spent in Australia and also Prof. Melo from Universidade Federal do Paraná for the chemical and DXRD analyses. A special acknowledgement is made to the staff of the Centre of Microscopy and Microanalysis of UWA for their support during the microscopy analysis. Finally, we acknowledge Dr Peter C. Ryan, Prof. José Torrent and Prof. Helge Stanjek for their valuable suggestions on the first version of this paper.

REFERENCES

Barnhisel, R.I. and Bertsch, P.M. (1989) Chlorites and hydroxy-interlayered vermiculite and smectite. Pp. 730–779 in: *Minerals in Soil Environments* (J.B. Dixon and S.B. Weed, editors). Soil Science Society of America, Madison, Wisconsin.

Bergkraut, V., Singer, A. and Stahr, K. (1994) Palagonite reconsidered: Paracrystalline illite:smectites from regoliths on basic pyroclastics. *Clays and Clay Minerals*, **42**, 582–592.

Birkenmajer, K. (2001) Retreat of the Ecology Glacier, Admiralty Bay, King George Island (South Shetland Islands, West Antarctica), 1956–2001. *Bulletin of the Polish Academy of Sciences. Earth Sciences*. **50**, 16–29.

Blume, H.P., Beyer, L., Kalk, E. and Kuhn, D. (2002) Weathering and soil formation. Pp. 114–138 in: *Geoecology of Antarctic Ice-Free Coastal Landscapes* (L. Beyer and M. Bölter, editors). Spinger-Verlag, Berlin.

Blume, H.P., Chen, J., Kalk, E. and Kuhn, D. (2004) Mineralogy and weathering of Antarctic Cryosols. Pp. 415–426 in: *Cryosols – Permafrost Affected Soils* (J. Kimble, editor). Springer-Verlag, Berlin.

Bockheim, J.G. and Tarnocai, C. (1998) Recognition of cryoturbation for classifying permafrost-affected soils. *Geoderma*, **81**, 281–293.

Borchardt, G. (1989) Smectites. Pp. 675–718 in: *Minerals in Soil Environments* (J. B. Dixon and S.B. Weed, editors). Soil Science Society of America, Madison, Wisconsin.

Brindley, G.W and Brown, G. (1980) *Crystal Structures of Clay Minerals and their X-ray Identification*. Monograph **5**, Mineralogical Society, London.

Campbell, I.B and Claridge, G.G.C. (1987) *Antarctica: Soils, Weathering Processes and Environment*. Elsevier, Amsterdam, 368 pp.

Campbell, I.B and Claridge, G.G.C. (2004a) Cryosols in the extremely arid Transarctic Mountains Region of Antarctica. Pp. 391–414 in: *Cryosols – Permafrost Affected Soils* (J. Kimble, editor). Springer-Verlag, Berlin.

Campbell, I.B and Claridge, G.G.C. (2004b) Weathering processes in arid Cryosols. Pp. 447–458 in: *Cryosols – Permafrost Affected Soils* (J. Kimble, editor). Springer-Verlag, Berlin.

Campbell, A.S. and Schwertmann, U. (1985) Evaluation of selective dissolution extractants in soil chemistry and mineralogy by differential X-ray diffraction. *Clay Minerals,* **20**, 515–519.

Dahlgren, R.A. (1994) Quantification of allophane and imogolite. Pp. 430–448 in: *Quantitative Methods in Soil Mineralogy* (J.E. Amonette and L.W. Zelazny, editors). Soil Science Society of America, Madison, Wisconsin.

Doner, H.E. and Lynn, W.C. (1989) Carbonates, Halide, Sulfate, and Sulfide Minerals. Smectite. Pp. 279–324 in: *Minerals in Soil Environments* (J.B. Dixon and S.B. Weed, editors). Soil Science Society of America, Madison, Wisconsin.

Drees, L.R., Wilding, L.P., Smeck N.E. and Senkayi, A.L. (1989) Silica in soils: quartz and disordered silica polymorphs. Pp. 914–965 in: *Minerals in Soil Environments* (J.B. Dixon and S.B. Weed, editors). Soil Science Society of America, Madison.

Egli, M., Mirabella, A. and Fitze, P. (2001) Clay mineral formation in soils of two different chronosequences in the Swiss Alps. *Geoderma,* **104**, 145–175.

EMBRAPA – Centro Nacional de Pesquisa de Solos (1997) *Manual de métodos de análise de solo*. Centro Nacional de Pesquisa de Solos, Rio de Janeiro, 212 pp.

Farmer, V.C., Fraser, A.R. and Tait, J.M. (1979) Characterization of the chemical structures of natural and synthetic aluminosilicate gels and sols by infrared spectroscopy. *Geochimica et Cosmochimica Acta*, **43**, 1417–1420.

Gardolinski, J.E., Wypych, F. and Cantão, M.P. (2001) Esfoliação e hidratação da caulinita após intercalação com

ureia. *Química Nova*, **24**,767–775.
Gee, G.W. and Bauder, J.W. (1986) Particle-size analysis. Pp. 383–412 in: *Methods of Soil Analysis, Part 1: Physical and Mineralogical Methods* (A. Klute, editor). Soil Science Society of America, Madison, Wisconsin.
Jackson, M.L. (1979) *Soil Chemical Analysis – Advanced Course*. Prentice-Hall, Madison, Wisconsin, 895 pp.
Jackson, M.L., Lim, C.H. and Zelazny, L.W. (1986) Oxides, hydroxides, and aluminosilicates. Pp. 101–150 in: *Methods of Soil Analysis Part 1: Physical and Mineralogical Methods* (A. Klute, editor). Soil Science Society of America, Madison, Wisconsin.
Jeong, G.Y. and Yoon, H.I. (2001) The origin of clay minerals in soils of King George Island, South Shetlands Islands, West Antarctica, and its implications for the clay-mineral composition of marine sediments. *Journal of Sedimentary Research*, **71**, 833–842.
Kelly, W.C. and Zumberge, J.H. (1961) Weathering of a quartz diorite at Marble Point, McMurdo Sound, Antarctica. *Journal of Geology,* **69**, 433–446.
Melo, V.F., Novais, R.F., Schaefer, C.E.G.R., Fontes, M.P.F. and Singh, B. (2002a) Mineralogia das frações areia, silte e argila de sedimentos do Grupo Barreiras no município de Aracruz, estado do Espírito Santo. *Revista Brasileira de Ciência do Solo*, **26**, 22–35.
Melo, V.F., Schaefer, C.E.G.R., Novais, R.F., Singh, B. and Fontes, M.P.F. (2002b) Potassium and magnesium in clay minerals of some Brazilian soils as indicated by a sequential extraction procedure. *Communication in Soil Science and Plant Analysis*, **33**, 2203–2225.
Myrcha, A., Pietr, S.J. and Tatur, A. (1985) The role of pygoscelid penguin rookeries in nutrient cycles at Admiralty Bay, King George Island. Pp. 156–163 in: *Antarctic Nutrient Cycles and Food Webs* (W.R. Siegfried, P.R. Condy and R.M. Laws, editors). Springer-Verlag, Berlin.
Nriagu, J.O. and Moore, P.B. (1984) *Phosphate Minerals*. Springer-Verlag, Berlin, 442 pp.
Ostroumov, V. (2004) Physico-chemical processes in cryogenic soils. Pp. 347–365 in: *Cryosols – Permafrost Affected Soils* (J. Kimble, editor). Springer-Verlag, Berlin.
Parfitt, R.L. (1990) Allophane in New Zealand – a review. *Australian Journal of Soil Research*, **28**, 343–360.
Parfitt, R.L. and Kimble, J.M. (1989) Conditions for formation of allophane in soils. *Soil Science Society of America Journal*, **53**, 971–977.
Parfitt, R.L. and Wilson, A.D. (1985) Estimation of allophane and halloysite in three sequences of volcanic soils, New Zealand. *Catena Supplement*, **7**, 1–8.
Sawhney, B.L. (1989) Interstratification in layer silicates. Pp. 789–824 in: *Minerals in Soil Environments* (J.B. Dixon and S.B. Weed, editors). Soil Science Society of America, Madison, Wisconsin.
Schulze, D.G. (1994) X-ray diffraction analysis of soil minerals. Pp. 412–429 in: *Quantitative Methods in Soil Mineralogy* (J. E. Amonette and L.W. Zelazny, editors). Soil Science Society of America, Madison, Wisconsin.
Schwertmann, U. (1973) Use of oxalate for Fe extraction from soils. *Canadian Journal of Soil Science*, **53**, 244–246.
Simas, F.N.B., Schaefer, C.E.R.G., Albuquerque Filho, M.R., Melo, V.F., Michel, R.F.M., Pereira, V.V. and Gomes, M.R.M. (2005) Pedogenesis and selected mineralogical and micropedological attributes of ornithogenic Cryosols in Maritime Antarctica: phosphatization as a soil-forming process. *Geoderma* (in review).
Smith, B.F.L. (1994) Characterization of poorly ordered minerals by selective chemical methods. Pp. 333–353 in: *Clay Mineralogy: Spectroscopic and Chemical Determinative Methods* (M.J. Wilson, editor). Chapman & Hall, London.
Środoń, J. and Eberl, D.D. (1984) Illite. Pp. 495–539 in: *Micas* (S.W. Bailey, editor). Reviews in Mineralogy, **13**. Mineralogical Society of America, Washington, D.C.
Tan, K.B., Hajek, B.F. and Barshad, I. (1986) Thermal analysis techniques. Pp. 151–183 in: *Methods of Soil Analysis - Part I: Physical and Mineralogical Methods* (A. Klute, editor). Soil Science Society of America, Madison, Wisconsin.
Tatur, A. (1989) Ornithogenic soils of the maritime Antarctic. *Polish Polar Research*, **4**, 481–532.
Tatur, A. and Barczuk, A. (1985) Ornithogenic phosphates on King George Island, Maritime Antarctic. Pp. 163–169 in: *Antarctic Nutrient Cycles and Food Webs* (W.R. Siegfried, P.R. Condy and R.M. Laws, editors). Springer-Verlag, Berlin.
Tatur, A. and Myrcha, A. (1993) Ornithogenic soils. Pp. 161–165 in: *The Antarctic Coastal Ecosystem of Admiralty Bay* (S. Rakusa-Suszczewski, editor). Polish Academy of Sciences, Warsaw.
Tatur, A., Myrcha, A. and Niegodzisz, J. (1997) Formation of abandoned penguin rookery ecosystems in the maritime Antarctic. *Polar Biology*, **17**, 405–417.
Van Vliet-Lanoë, B., Fox, C.A. and Gubin, S.V. (2004) Micromorphology of Cryosols. Pp. 365–391 in: *Cryosols – Permafrost-affected Soils* (J.M. Kimble, editor). Springer-Verlag, Berlin.
Wada, K. (1989) Allophane and imogolite. Pp. 1052–1081 in: *Minerals in Soil Environments* (J.B. Dixon and S.B. Weed, editors). Soil Science Society of America, Madison, Wisconsin.
Wilson, M.J. (1999) The origin and formation of clay minerals in soils: past, present and future perspectives. *Clay Minerals*, **34**, 7–25.
Yeomans, J.C. and Bremner, J.M. (1988) A rapid and precise method for routine determination of organic carbon in soil. *Communications in Soil Science and Plant Analysis*, **19**, 1467–1476.
Yong, I.L., Lim, H.S and Yoon, H.I. (2004) Geochemistry of soils of King George Island, South Shetlands Islands, West Antarctica: Implications for pedogenesis in cold polar regions. *Geochimica et Cosmochimica Acta*, **68**, 4319–4333.
Yoshinaga, N. (1986) Mineralogical characteristics. II. Clay minerals. Pp. 41–56 in: *Ando Soils in Japan* (K. Wada, editor). Kyushu University Press, Japan.

(*Received 2 February 2006; revised 2 August 2006; Ms. 1137; A.E. Helge Stanjek*)